AD_____

Award Number: DAMD17-00-1-0403

TITLE: Impact of Disrupted BRCA2 Protein-Protein Interactions on DNA Repair and Tumorigenesis

PRINCIPAL INVESTIGATOR: Christopher J. Sarkisian

CONTRACTING ORGANIZATION: University of Pennsylvania
Philadelphia, PA 19104-3246

REPORT DATE: July 2003

TYPE OF REPORT: Annual Summary

PREPARED FOR: U.S. Army Medical Research and Materiel Command
Fort Detrick, Maryland 21702-5012

DISTRIBUTION STATEMENT: Approved for Public Release;
Distribution Unlimited

The views, opinions and/or findings contained in this report are those of the author(s) and should not be construed as an official Department of the Army position, policy or decision unless so designated by other documentation.

REPORT DOCUMENTATION PAGE

Form Approved
OMB No. 074-0188

1. AGENCY USE ONLY (Leave blank)	2. REPORT DATE	3. REPORT TYPE AND DATES COVERED
	July 2003	Annual Summary (1 Jul 2000 - 30 Jun 2003)

4. TITLE AND SUBTITLE

Impact of Disrupted BRCA2 Protein-Protein Interactions on DNA Repair and Tumorigenesis

5. FUNDING NUMBERS

DAMD17-00-1-0403

6. AUTHOR(S)

Christopher J. Sarkisian

7. PERFORMING ORGANIZATION NAME(S) AND ADDRESS(ES)

University of Pennsylvania
Philadelphia, PA 19104-3246

E-Mail: csarkisi@mail.med.upenn.edu

8. PERFORMING ORGANIZATION REPORT NUMBER

9. SPONSORING / MONITORING AGENCY NAME(S) AND ADDRESS(ES)

U.S. Army Medical Research and Materiel Command
Fort Detrick, Maryland 21702-5012

10. SPONSORING / MONITORING AGENCY REPORT NUMBER

11. SUPPLEMENTARY NOTES

12a. DISTRIBUTION / AVAILABILITY STATEMENT

Approved for Public Release; Distribution Unlimited

12b. DISTRIBUTION CODE

13. ABSTRACT (Maximum 200 Words)

In this report, we have investigated the effects of overexpression of active Ras within the mammary epithelium. Using the tetracycline-inducible system, we have generated a line of mice which, when also bearing rtTA transgene expressed under control of the MMTV LTR, inducibly express active H-Ras in the mammary epithelium in response to the drug doxycycline. We have also shown that pathways downstream of Ras are activated, such as the Raf/MEK/MAPK pathway. We have shown that the mammary epithelium undergoes an increase in proliferation in response to Ras, but undergoes a proliferative arrest and inhibition of ductal elongation in chronically induced glands. This arrest occurs in the absence of increased apoptosis. Removal of doxycycline abrogates the growth arrest and restores a normal gland within 60 days. Finally, the p19/p53/p21 pathway is activated in response to Ras.

14. SUBJECT TERMS

Breast Cancer

15. NUMBER OF PAGES

24

16. PRICE CODE

17. SECURITY CLASSIFICATION OF REPORT	18. SECURITY CLASSIFICATION OF THIS PAGE	19. SECURITY CLASSIFICATION OF ABSTRACT	20. LIMITATION OF ABSTRACT
Unclassified	Unclassified	Unclassified	Unlimited

Table of Contents

Christopher J. Sarkisian
627 BRB2/3
421 Curie Blvd
Philadelphia, PA 19104

The goals of my 1999 pre-doctoral fellowship "Role Of *Brca2* In Cell Cycle Progression And The Response To DNA Damage In Mammary Epithelial Cells", were to 1) Determine whether Brca1 and Brca2 interact in murine cells; 2) Map the domain(s) of Brca2 necessary for such an interacting with Brca1; and 3) Determine whether mice bearing a *Brca2* allele defective in binding to Brca1 are susceptible to genetic instability and/or tumorigenesis. We have published results addressing aims 1 and 2 in the manuscript, "Analysis Of Murine Brca2 Reveals Conservation Of Protein-Protein Interactions But Differences In Nuclear Localization Signals" (Appendix 1). In this manuscript, we have demonstrated that Brca2 and Brca1 interact in murine cells (Fig 4, Appendix 1). We have also shown that the amino terminus of murine Brca2 is sufficient to interact with human BRCA1 (Fig 6, Appendix 1).

However, as mentioned in my previous annual report, inefficient expression of epitope-tagged constructs of *Brca2*, and our lack of antisera to the carboxyl-terminus of murine Brca2, have prevented us from determining whether the amino- terminus of Brca2 is required for interaction with Brca1. Furthermore, mapping of the Brca2-Brca1 interaction using GST pulldown techniques has not been possible due to difficulties in the purification of several GST-Brca2 fusion proteins. These complications have precluded the completion of Specific Aims 2 and 3 of the Statement of Work. For these reasons, we chose to address an alternate problem in breast cancer research.

INTRODUCTION

The small GTPase protein Ras is one of the most commonly mutated genes in human cancers. Over 20% of human cancers harbor activating mutations in one of three Ras family members, H-, K-, or N-Ras(1). Ras is a signal transducer known to be downstream from numerous cell surface receptors, among them molecules implicated in breast cancer such as the EGFR and erbB2 receptor tyrosine kinases(2,3). Stable transfection of Ras into NIH3T3 cells will transform them into malignant sarcomas, and female mice constitutively expressing activated H-Ras under the control of the MMTV promoter develop mammary carcinomas(4,5). Blockade of Ras signaling, in contrast, is inhibitory to cell growth in cultured cell lines and can inhibit tumor growth in vivo(6,7).

In direct contrast to results obtained using immortalized cell lines, retroviral infection of Ras into primary murine embryonic fibroblasts (MEFs) has been shown to induce a short period of proliferation, followed by a growth arrest that shares many features with cellular senescence(8). Moreover, the growth arrest activated by Ras has also been shown to require functional p53 and INK4a/ARF pathways(8). The genetic loci encoding these proteins are the two most commonly mutated loci in human cancers, suggesting the mechanism underlying Ras-induced growth arrest may be an essential tumor suppressive mechanism present within cells.

Normal MEFs cultured *in vitro* arrest growth prior to telomere dysfunction, thought to be due to genotoxic stress arising from hyperoxic culture conditions(9). The senescent-like phenotype caused by Ras overexpression in primary cells also occurs with normal telomere function(10,11). It is therefore fair to question whether Ras-induced growth arrest in fact represents an innate protective mechanism against the activation of a potent oncogene, or merely the extension of an artifact of *in vitro* culture conditions. To address this requires the overexpression of Ras in somatic tissues *in vivo*, and the determination of whether any senescent response occurs in the cells expressing Ras. We have generated a line of mice capable of inducibly overexpressing activated H-Ras within the mammary epithelium. Using this line of mice we will determine if growth arrest and/or apoptosis occurs in the mammary epithelium in response to activation of Ras. We will also determine if markers of senescence are detectable in Ras-expressing cells. Finally, we will breed MTB/TRAS mice to p53 knockout mice to determine if a p53-dependent growth arrest occurs in response to Ras.

BODY

The goals of my pre-doctoral fellowship "Determination of a Senescent of Response to Oncogenic Ras Mutation *in Vivo*", are to 1) Generate a line of mice inducibly expressing activated Ras within the mammary epithelium, 2) Characterize the proliferative, apoptotic, and senescent responses of mammary epithelial cells to activated H-Ras, and 3) Determine if the phenotype induced by activated H-Ras is dependent on p53.

We have previously generated a line of mice, designated MTB, which express the reverse tetracycline dependent transactivator (rtTA) under control of the mouse mammary tumor virus (MMTV) LTR(12). MTB female mice express rtTA within the mammary epithelium and salivary gland but in no other organs(12). We have also generated a line of mice harboring a transgene that expresses viral activated H-Ras under control of the tetracycline operon, called the TRAS line of mice. The transcript expressing *H-Ras* also contains an IRES-*Luciferase* cassette such that Luciferase expression may be used as a surrogate for transgene expression. In response to the drug doxycycline (dox), bitransgenic MTB/TRAS mice have a large induction of luciferase activity in the mammary gland while uninduced and uninduced bitransgenic mice express luciferase levels near those of control monotransgenic mice (data not shown). Luciferase activity was detectable at such levels only within the mammary and salivary glands (data not shown). We therefore conclude that the MTB/TRAS system represents a useful way to specifically and inducibly express H-Ras within the mammary epithelium.

MTB/TRAS mice rapidly and inducibly express *v- H-RAS* within the mammary gland at the RNA and protein levels in response to doxycycline (Fig 1 and data not shown). Specifically precipitating the GTP-bound form of Ras, which is the active form of Ras, demonstrates that while total levels of Ras increase only several fold in response to dox, the levels of GTP-bound Ras increase dramatically in response to dox (Fig 1A-B). Moreover, immunoblots for phospho-MEK, a kinase activated as part of the MAP kinase pathway downstream of Ras, demonstrated that this pathway is activated within 24 hrs of Ras activation by dox (Fig 1B). We conclude that MTB/TRAS mice express a biologically active form of H-Ras in response to doxycycline.

To determine whether mammary epithelial cells undergo a proliferative arrest in response to induction of Ras, we performed co-immunofluorescence of BrdU with cytokeratin 18, a marker for luminal epithelial cells that express the Ras transgene (data not shown). Quantitation of proliferative rates demonstrated that

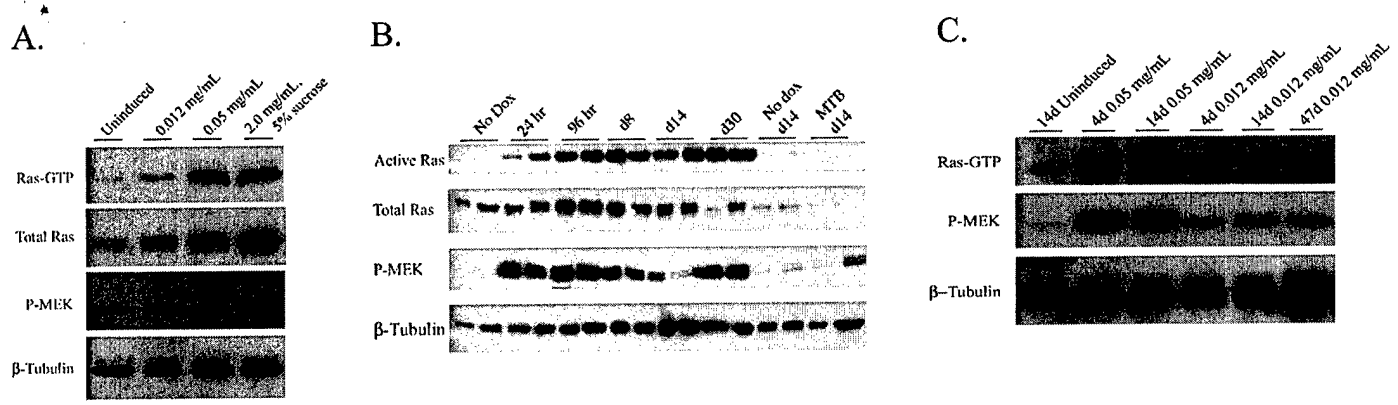

Figure 1 –Immunoblots against the indicated proteins were performed on mammary gland extracts from (A) 96 hr inductions of MTB/TRAS mice with specified doses of dox. (B) Time course of MTB/TRAS mice induced at 0.05 mg/mL dox. (C) MTB/TRAS mice induced at 0.05 mg/mL or 0.012 mg/mL dox for the indicated times.

MTB/TRAS mammary epithelial cells experience a rapid increase in proliferation following induction with 2.0 mg/mL dox, but also that proliferation rates decrease to levels near uninduced mice upon long term inductions (Fig 2A). We find a statistically significant difference in proliferation rates of MTB/TRAS mammary epithelial cells induced for 48 hours at 2.0 mg/mL dox compared to those induced for 14 days at 2.0 mg/mL dox ($p=0.006$). Immunoblots for active Ras and phospho-MEK on short term and long term induced tissue have demonstrated that this decrease in proliferation is not due to a decrease in Ras activity during the induction (Fig 1C). Transplants of MTB/TRAS mammary glands onto wild type or monotransgenic hosts have demonstrated that this growth arrest is gland autonomous (data not shown). Furthermore this decrease in proliferation occurs in the absence of an increase in apoptosis (Fig 2B). Finally, in contrast to high dose induction of Ras, when Ras is induced at a lower dose of doxycycline (0.012 mg/mL dox) we observe a low level of mammary epithelial cell proliferation that persists even after 47 days of induction (Fig 2A). We conclude that induction of high dose, but not low dose, Ras activity initiates an *in vivo* growth arrest program in mammary epithelial cells.

One of the hallmarks of Ras-induced growth arrest in fibroblasts is that activation of the p53 tumor suppressor occurs due to induction p19ARF, an inhibitor of Mdm2, which in turn acts as an ubiquitin ligase for p53. We wished to determine if these proteins were activated in response to H-Ras. Immunoblots for p16, p19, p53 phospho-serine 15, and the p53 target gene p21WAF1/CIP1 show that the p53 pathway is indeed activated

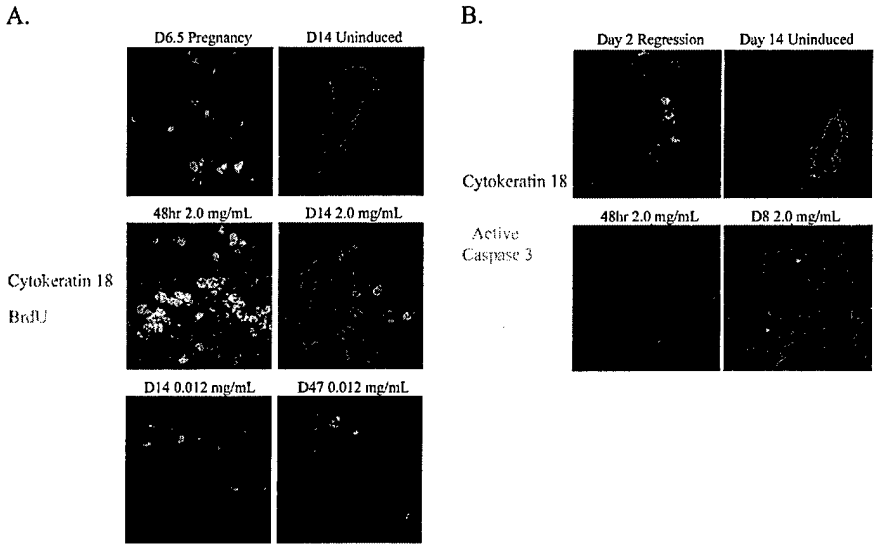

Figure 2 – MTB/TRAS mammary sections co-stained for cytokeratin 18 and BrdU (A) or active caspase 3 (B).

in the mammary epithelium, with maximal activation of the pathway occurring 8-14 days post-induction with dox (Fig 3). While we have observed increases in plasminogen activator inhibor-1 (PAI-1) mRNA in response to Ras, we have not detected appreciable levels of senescence-associated β-galactosidase activity in mammary glands (data not shown). We conclude that while key regulators of Ras-induced growth arrest increase in induced MTB/TRAS mammary glands, not all markers of senescence *in vitro* similarly increase.

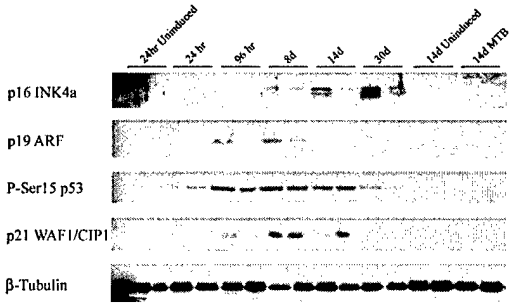

Figure 3 – Mammary gland extracts from MTB/TRAS mice induced at 0.05 mg/mL dox were immunoblotted against the indicated proteins of the p16 and p53 pathways.

Due to a decreased proportion of female FVB p53-/- mice relative to wild type and heterozygous females, as well as due to tumors that arise in viable p53 -/- females prior to induction with dox, we have been unable to generate sufficient numbers of MTB/TRAS/p53-/- female mice for determination of p53 dependence

of Ras-induced proliferative arrest. However, as neither telomere-dependent senescence nor Ras-induced growth arrest has been shown to be reversible *in vitro* when the initiating stimulus is removed, we wished to determine if the Ras-induced growth arrest could be reverted upon withdrawal of Ras expression. Chronically induced, growth arrested MTB/TRAS mammary glands were deinduced for 3, 7, 21, or 60 days and examined by carmine-stained wholemounts to determine whether the proliferative arrest and inhibition of ductal elongation could be abrogated. We observed a complete restoration of the epithelial tree by day 60 of deinduction (Fig 4A). Co-immunofluorescence of cytokeratin 18 and BrdU determined that an increase in proliferation of mammary epithelial cells occurs upon deinduction, peaking at 7 days post-deinduction, and resuming quiescence upon days 21-60 (Fig 4B). We conclude that Ras-induced proliferative arrest and inhibition of ductal elongation are reversible.

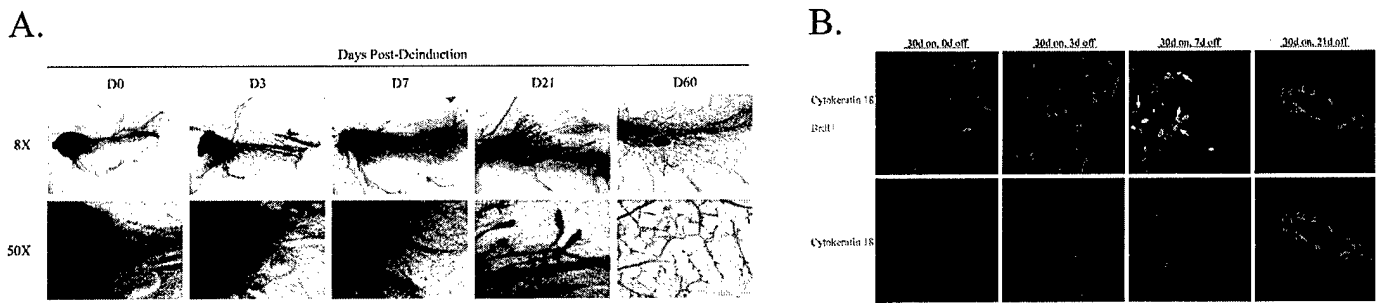

Fig 4 – (A) Chronically induced MTB/TRAS mammary glands were deinduced for the indicated time, stained with carmine's dye, and wholemounted for analysis of reversibility of Ras-induced growth arrest. (B) Deinduced glands were co-stained for cytokeratin 18 and BrdU using immunofluorescent microscopy.

STATEMENT OF WORK

Specific Aim 1. Generate a line of mice inducibly expressing activated Ras within the mammary epithelium: Months 12-24

1. Generate bitransgenic MTB/TRAS mice and verify tissue-specific response to doxycycline: Months 12-18
2. Determine doxycycline dose responsiveness of MTB/TRAS mice: Months 18-24
3. Verify that the MAP kinase pathway is activated in response to transgenic Ras: Months 18-24

Specific Aim 2. Characterize the proliferative, apoptotic, and senescent responses of mammary epithelial cells to activated H-Ras: Months 24-30

1. Characterize proliferative and apopotic rates in uninduced and induced MTB/TRAS mammary glands: Months 24-30
2. Determine activation of p53 and p19 pathways in uninduced and induced MTB/TRAS mammary glands: Months 24-30
3. Determine levels of PAI-1 and senescence-associated β-galactosidase activity in uninduced and induced MTB/TRAS mammary glands: Months 24-30

Specific Aim 3. Determine if the phenotype induced by activated v-H-Ras is dependent on p53: Months 30-36

1. Generate MTB/TRAS/p53-/- and MTB/TRAS/p53+/+ female mice: Months 30-36
2. Induce above mice for 0, 4, and 14 days, and compare carmine stained whole mounts and H & E sections for gross differences in morphology: Months 30-36
3. Determine proliferation and apoptotic rates in induced MTB/TRAS/p53-/- and MTB/TRAS/p53+/+ mammary glands: Months 30-36

KEY RESEARCH ACCOMPLISHMENTS

- MTB/TRAS female mice inducibly express active H-Ras within the mammary and salivary glands
- The MAP kinase pathway is activated in response to Ras in mammary glands from MTB/TRAS mice
- Mammary glands from MTB/TRAS mice induced to express H-Ras develop dramatic increases in epithelial cell number based on gross morphology and histologic stains
- Activation of Ras induces a transient increase in proliferation followed by a growth arrest and inhibition of ductal elongation.
- Ras-induced proliferative arrest occurs in the absence of increased apoptosis
- Unlike high dose induction of Ras, low dose induction of Ras in the mammary gland does not result in a decrease in cellular proliferation.
- Ras-induced growth arrest and inhibition of ductal elongation are reversible upon deinduction of Ras
- The p16/p19/p53 pathway is activated in response to Ras in mammary glands from MTB/TRAS mice

REPORTABLE OUTCOMES

Sarkisian CJ, Master SR, Huber LJ, Ha SI, Chodosh LA "Analysis of murine Brca2 reveals conservation of protein-protein interactions but differences in nuclear localization signals" J Biol Chem 2001 276: 37640-8 (Appendix 1)

CONCLUSIONS

We have generated a bitransgenic system whereby the effects of activation of a potent oncogene, *v-H-Ras*, within the adult mammary epithelium may be determined. MTB/TRAS mice specifically and inducibly express activated H-Ras within mammary epithelia of MTB/TRAS mice, but not in uninduced bitransgenics or monotransgenic mice. Furthermore, we have demonstrated the the Ras transgene expressed is biologically active, in that the MAP kinase pathway is activated in response to Ras induction. In addition to the MAP kinase pathway, we have also shown that the p53 pathway is activated in response to this oncogene, as also occurs in MEFs in vitro. We have demonstrated that there is an initial response of epithelial proliferation in response to Ras, but that long term inductions of Ras actually lead to a growth arrest following this proliferative increase. Furthermore, this proliferative arrest is accompanied by an inhibitition of ductal elongation. Interestingly, we did not detect a decrease in proliferation or an inhibition in ductal elongation when Ras was induced at a lower concentration of dox. The proliferation decrease and inhibition to ductal elongation has been shown to be mammary gland autonomous, indicating that the effects observed are not due to expression of Ras in the salivary gland or other organs. We did not detect a significant increase in apoptosis in response to Ras in either short term or long term inductions, suggesting that the decrease in proliferation is not due to programmed cell death of Ras expressing cells.

We have additionally shown that the proliferative arrest following chronic induction of Ras is reversible upon removal of Ras signalling. Ablation of Ras signalling restores ductal elongation, permitting re-formation of the epithelial tree. This occurs by resumption of proliferation of mammary epithelial cells during the reversal of ductal elongation. This demonstrates the dependency of the proliferative arrest upon maintenance of Ras signalling. We have shown that accompanying the growth arrest is an increase in the p53 and p16 tumor suppressor pathways, suggesting that these pathways may be mediating the proliferative arrest in chronically induced glands. These molecules have previously been demonstrated to play roles in regulating cellular senescence. However, examination of markers for senescence in these mice, such as an increase in *PAI-1* RNA and in senescent-associated β-galactosidase activity(13,14), showed that the growth arrest appears to have some but not all characteristics of fibroblast senescence *in vitro*. Future experiments will cross MTB/TRAS mice with mice lacking the tumor suppressor *p19 ARF* or expressing a dominant negative *p53* allele, to determine whether molecules shown to regulate Ras-induced growth arrest *in vitro* are also required for arrest *in vivo*.

REFERENCES

1. Bos, J. L. (1989) *Cancer Res* **49**, 4682-9
2. Deuel, T. F. (1987) *Annual Review of Cell Biology* **3**, 443-92
3. Galang, C. K., Garcia-Ramirez, J., Solski, P. A., Westwick, J. K., Der, C. J., Neznanov, N. N., and Oshima, R. G. H., C.A. (1996) *Journal of Biological Chemistry* **271**, 7992-8
4. McCoy, M. S., Toole, J. J., Cunningham, J. M., Chang, E. H., Lowy, D. R., and Weinberg, R. A. (1983) *Nature* **302**, 79-81
5. Sinn, E., Muller, W., Pattengale, P., Tepler, I., Wallace, R., and Leder, P. (1987) *Cell* **49**, 465-75
6. Sun, J., Qian, Y., Hamilton, A. D., and Sebti, S. M. (1995) *Cancer Research* **55**, 4243-7
7. Tokumitsu, Y., Nakano, S., Ueno, H., and Niho, Y. (2000) *Journal of Cellular Physiology* **183**, 221-7
8. Serrano, M., Lin, A. W., McCurrach, M. E., Beach, D., and Lowe, S. W. (1997) *Cell* **88**, 593-602
9. Sherr, C. J., and DePinho, R. A. (2000) *Cell* **102**, 407-10
10. Jones, C. J., Kipling, D., Morris, M., Hepburn, P., Skinner, J., Bounacer, A., Wyllie, F. S., Ivan, M., Bartek, J., Wynford-Thomas, D., and Bond, J. A. (2000) *Molecular & Cellular Biology* **20**, 5690-9
11. Wei, S., Wei, S., and Sedivy, J. M. (1999) *Cancer Research* **59**, 1539-43
12. Gunther, E. J., Belka, G. K., G.B., W., Wang, J., Hartman, J. L., Boxer, R. B., and Chodosh, L. A. (2002) *FASEB Journal* **16**, 283-92
13. Ferbeyre, G., de Stanchina, E., Querido, E., Baptiste, N., Prives, C., and Lowe, S. W. (2000) *Genes & Development* **14**, 2015-27
14. Pearson, M., Carbone, R., Sebastiani, C., Cioce, M., Fagioli, M., Saito, S., Higashimoto, Y., Appella, E., Minucci, S., Pandolfi, P. P., and Pelicci, P. G. (2000) *Nature* **406**, 207-10

Appendix Cover Sheet

THE JOURNAL OF BIOLOGICAL CHEMISTRY
Vol. 276, No. 40, Issue of October 5, pp. 37640–37648, 2001
Printed in U.S.A.

Analysis of Murine Brca2 Reveals Conservation of Protein-Protein Interactions but Differences in Nuclear Localization Signals*

Received for publication, July 5, 2001, and in revised form, July 23, 2001
Published, JBC Papers in Press, July 26, 2001, DOI 10.1074/jbc.M106281200

Christopher J. Sarkisian‡, Stephen R. Master‡, L. Julie Huber‡, Seung I. Ha‡ and Lewis A. Chodosh‡§¶

From the ‡Department of Molecular and Cellular Engineering and §Division of Endocrinology, Diabetes and Metabolism, University of Pennsylvania School of Medicine, Philadelphia, Pennsylvania 19104-6160

In this report, we have analyzed the protein encoded by the murine *Brca2* locus. We find that murine Brca2 shares multiple properties with human BRCA2 including its regulation during the cell cycle, localization to nuclear foci, and interaction with Brca1 and Rad51. Murine Brca2 stably interacts with human BRCA1, and the amino terminus of Brca2 is sufficient for this interaction. Exon 11 of murine Brca2 is required for its stable association with RAD51, whereas the carboxyl terminus of Brca2 is dispensable for this interaction. Finally, in contrast to human BRCA2, we demonstrate that carboxyl-terminal truncations of murine Brca2 localize to the nucleus. This finding may explain the apparent inconsistency between the cytoplasmic localization of carboxyl-terminal truncations of human BRCA2 and the hypomorphic phenotype of mice homozygous for similar carboxyl-terminal truncating mutations.

Women inheriting mutations in the *BRCA2* tumor-suppressor gene have up to an 84% lifetime risk of developing breast cancer (1), and these tumors account for ~35% of inherited breast cancers in women (2). *BRCA2* encodes a 3418-amino acid nuclear protein of a predicted molecular mass of 384 kDa. Most disease-causing *BRCA2* alleles contain truncating mutations that result in deletion of the three characterized nuclear localization signals present at the extreme carboxyl terminus of BRCA2 (3, 4). Because these signals are required for the nuclear localization of human BRCA2, it has been postulated that truncating alleles of *BRCA2* are functionally equivalent to null alleles of this tumor suppressor gene (3).

Though its exact cellular role remains unclear, a growing body of evidence indicates that BRCA2 is involved in DNA damage-response pathways shared with BRCA1 and RAD51. BRCA2, BRCA1, and RAD51 are each co-regulated with highest levels of expression occurring during the S and G_2/M phases of the cell cycle, and these proteins co-localize to discrete foci within the nucleus (5–11). Furthermore, human BRCA2 has been shown to physically interact with both RAD51 (12–16) and BRCA1 (16).

* This work was supported in part by NCI, National Institutes of Health Grants CA71513 and CA78410 and by United States Army Breast Cancer Research Program Grants DAMD17-00-1-0403 (to C. J. S.), DAMD17-98-1-8230 (to L. J. H.), and DAMD17-98-1-8226 (to L. A. C.). The costs of publication of this article were defrayed in part by the payment of page charges. This article must therefore be hereby marked "*advertisement*" in accordance with 18 U.S.C. Section 1734 solely to indicate this fact.

¶ To whom correspondence should be addressed: Dept. of Molecular and Cellular Engineering, 612 Biomedical Research Building II/III, University of Pennsylvania School of Medicine, 421 Curie Blvd., Philadelphia, PA 19104–6160. Tel.: 215-898-1321; Fax: 215-573-6725; E-mail: chodosh@mail.med.upenn.edu.

Human BRCA2 binds to RAD51 via eight BRC repeats, each 30–80 amino acids in length, that are located within exon 11 of BRCA2 (17, 18). These repeats have been demonstrated by yeast two-hybrid analysis to be both necessary and sufficient for stable binding of human BRCA2 to RAD51 (12, 14, 15). The region(s) of BRCA2 that are required for binding to BRCA1 have been less clearly defined, though the carboxyl-terminal third of BRCA2 has been shown to be dispensable for this interaction (16). Nevertheless, despite the identification of BRCA2-RAD51 and BRCA2-BRCA1 protein-protein interactions, the contribution of these interactions to the tumor-suppressor functions of BRCA2 remains uncertain.

Mice bearing homozygous mutations in *Brca2* that yield truncations of all eight BRC repeats uniformly die *in utero* between embryonic day 6.5-8.5, with elevated levels of p53 and p21 (19–21). Notably, this phenotype is similar to that of mice homozygous for null mutations in either *Rad51* or *Brca1* (22–26). Whereas mice bearing truncating alleles of *Brca2* that remove only a subset of BRC repeats also die *in utero*, a fraction of homozygotes survive to birth with the survival rate being roughly proportional to the number of BRC repeats left intact (27–29). Surviving homozygotes invariably succumb to thymic lymphomas, and cells from these mice exhibit increased genotoxin sensitivity and chromosomal instability, as well as an impaired ability to form Rad51 nuclear foci in response to DNA damage (27–30). In contrast, mice homozygous for truncating mutations in *Brca2* that leave exon 11 intact exhibit a more limited sensitivity to genotoxins, are 100% viable, and do not appear to develop spontaneous tumors (31). These data argue for a central role of exon 11 in the genomic surveillance and tumor-suppressor functions of Brca2.

Whereas murine knockout models support a role for BRCA2 as a tumor suppressor, the increasingly severe defects observed in mice as larger amounts of the Brca2 carboxyl terminus are truncated appear inconsistent with reports that even small carboxyl-terminal truncations in human BRCA2 result in its cytoplasmic localization. That is, essentially all truncating alleles might be expected to behave similarly to null alleles, because carboxyl-terminal truncation would ostensibly lead to cytoplasmic localization and preclude Brca2 from participating in nuclear functions (3, 4). This apparent discrepancy could be because of differences in the subcellular localization signals of human and murine Brca2 or to differences in the functions of murine and human BRCA2 in the cytoplasm. In this regard, another apparent functional difference between murine and human BRCA2 is suggested by the mapping of a murine Brca2-Rad51 interaction to the carboxyl terminus of murine Brca2, because similar approaches have shown that the corresponding region of human BRCA2 lacks significant affinity for RAD51 (12, 14, 15). Further complicating the direct comparison of

murine and human BRCA2 is the fact that the overall amino acid homology between these orthologs is only 59%, a relatively low degree of evolutionary conservation compared with other tumor-suppressor genes. Together, these data have called into question the applicability of murine models for understanding the function of human BRCA2.

In this report, we characterize the murine Brca2 protein. We find that Brca2 stably interacts with murine Brca1 and Rad51. We demonstrate that the physical association of Brca2 with Rad51 requires exon 11 of murine Brca2 but not its carboxyl terminus. We also show that murine Brca2 differs from human BRCA2 in that carboxyl-terminal truncations of murine Brca2 localize to the nucleus. Collectively, our findings suggest that multiple functional interactions of Brca2 have been evolutionarily conserved with the notable exception of those signals required for its nuclear localization.

EXPERIMENTAL PROCEDURES

Isolation of Murine Brca2 cDNA—Poly(A)$^+$ RNA isolated from day 14 murine embryos was used to generate a cDNA library in lambda ZAP using the ZAP-cDNA synthesis and ZAP-cDNA Gigapack II Gold packaging kits according to manufacturer's instructions (Stratagene). 5×10^5 plaques from each library were screened by standard methods using [^{32}P]dCTP-labeled random-primed cDNA fragments (BMB) corresponding to nucleotides 2–221, 798–2932, and 9033–9972 of murine *Brca2*. Hybridization was performed at a concentration of 10^6 cpm/ml in 48% formamide, 10% dextran sulfate, 4.8× SSC, 20 mM Tris, pH 7.5, 10× Denhardt's solution, 20 μg/ml salmon sperm DNA, and 0.1% SDS at 42 °C overnight. Filters were washed twice in 2× SSC/0.1% SDS at room temperature for 20 min and twice in 0.2× SSC/0.1% SDS for 20 min at 50 °C and subjected to autoradiography on XAR-5 film (Eastman Kodak Co.). Phage clones were plaque purified, and plasmids were liberated by *in vivo* excision according to the manufacturer's instructions. Sequence analysis identified three overlapping clones that together spanned the entire *Brca2* coding sequence, with the exception of an internal deletion of nucleotides 454–672. This region was replaced with a polymerase chain reaction product generated from murine testis first-strand cDNA and primers 5′-GAATTCATGCCCGTTGAATACAAAAGGAGAC-3′ and 5′-CTCGAGGCAGATTTCCTCATTCTGGCTG-3′. After sequencing to verify the absence of additional mutations, the overlapping clones were assembled to generate a full-length murine *Brca2* cDNA.

Generation of Antisera—Using primers 5′-CATCCGAATTCTGCAGCACAGCGATTTAGGAC-3′ and 5′-CATCCCTCGAGGCACCGCAGAGTAAGAGGG-3′ (Brca2A), and 5′-CATCCGAATTCGATGAAGAAGCACGCAGCTC-3′ and 5′-CATCCCTCGAGACTGCATTTTTCACAGTGGC-3′ (Brca2B), polymerase chain reaction products corresponding to amino acids 19 to 135 (Brca2A) and 206 to 566 (Brca2B) were generated from a partial *Brca2* cDNA, ligated into pGEM-T vector (Promega), and subcloned in-frame into pGEX-6P-1 (Amersham Pharmacia Biotech). GST[1] fusion peptides were purified from BL21 *Escherichia coli* according to manufacturer's instructions. Brca2 peptides were cleaved from the GST domain using a site-specific protease, gel-purified by SDS-PAGE, and injected into rabbits using standard immunization protocols (Cocalico Biologicals). Sera from immunized rabbits were affinity-purified on columns containing immunogen bound to cyanogen bromide-activated Sepharose (Amersham Pharmacia Biotech) according to published methods (32).

Transfection of Cells—293T cells were transiently transfected using a standard calcium-phosphate protocol (33). For co-immunoprecipitation experiments, 2.5×10^6 cells on 150-mm dishes were transfected with 25 μg of DNA. For subcellular localization studies, 1×10^6 cells on 100-mm dishes were transfected with 5 μg DNA, and cells were split onto culture slides at 24 h post-transfection. All analyses were performed at 48 h post-transfection.

Cell Culture—All cells were grown at 37 °C in a humidified incubator supplemented with 5% CO_2. 293T, NMuMG, and 16MB9A cells were grown in Dulbecco's modified Eagle's medium supplemented with 10% bovine calf serum (Gem Cell), 2 mM L-glutamine, 100 units/ml penicillin, and 100 units/ml streptomycin. HC11 cells were cultured in RPMI supplemented with 10% bovine calf serum (Gem Cell), 1 mM L-glutamine, 100 units/ml penicillin, 100 units/ml streptomycin, 10 ng/ml epidermal growth factor, and 5 μg/ml insulin.

Immunoblotting and Immunoprecipitation—Cells were harvested by lysis in EBC Buffer (50 mM Tris, pH 8.0, 120 mM NaCl, 0.5% Igepal CA-630 (Sigma)), supplemented with phosphatase inhibitors (50 mM NaF and 1 mM β-glycerol phosphate) and protease inhibitors (100 μg/ml aprotinin, 10 μg/ml leupeptin, 10 μg/ml pefabloc). Following removal of insoluble debris by centrifugation, extracts were either boiled in 1× (final) Laemmli sample buffer (2% SDS, 10% glycerol, 60 mM Tris, pH 6.8, 5% β-mercaptoethanol, 250 mM dithiothreitol, 0.005% bromphenol blue) or subjected to immunoprecipitation. For immunoprecipitation studies, 1.0–1.5 mg of protein extract was incubated with 4 μg of affinity-purified antibody or, in the case of RAD51, 1 μl of polyclonal antiserum (Ab-1; Oncogene Science) for 1 h at 4 °C in a total volume of 1 ml of EBC plus inhibitors. Protein A-Sepharose (25 μl of a 50% slurry in PBS; Life Technologies, Inc.) was added, and incubation was continued for 1 h. The Sepharose beads were pelleted and washed three times in EBC plus inhibitors, resuspended, boiled in 14 μl of 2× (final) Laemmli sample buffer, and loaded for SDS-PAGE.

Except as noted, all protein samples were separated by 5% SDS-PAGE in 50 mM Tris base, 192 mM glycine, and 0.1% SDS. For immunoblotting, electrophoresed proteins were transferred onto nitrocellulose (Schleicher & Schuell) in 50 mM Tris base, 192 mM glycine, and 20% methanol in a submerged tank apparatus (Bio-Rad) for 12 h at 20 V. Blotted membranes were rinsed twice in PBS and blocked for 1 h at room temperature in PBS containing 5% nonfat milk and 0.05% Igepal CA-630 (MPBS-I). All affinity-purified rabbit polyclonal primary antibodies were used for immunoblotting at a final concentration of 2 μg/ml. Commercial antibodies, including anti-human BRCA2 Ab-2 (Oncogene Science), anti-RAD51 Ab-1 (Oncogene Science), anti-RAD51 Ab-1 (Neo-Markers), anti-BRCA1 MS110 (Oncogene Science), anti-β-tubulin N357 (Amersham Pharmacia Biotech), and anti-RAD50 R75020 (Transduction Laboratories) were used at the concentrations recommended by the manufacturer. Blots were incubated with primary antibodies diluted in MPBS-I for 1 h at room temperature and were subsequently washed three times in MPBS-I for 10 min each. Peroxidase-conjugated goat anti-rabbit or goat anti-mouse secondary antibodies (Jackson Immunoresearch) were incubated at a 1:5000 dilution for 1 h at room temperature in MPBS-I. Blots were washed three times in MPBS-I for 15 min each and rinsed four times with PBS, and antibody complexes were detected by chemiluminescence (ECL Plus; Amersham Pharmacia Biotech) on XAR-5 film (Kodak).

Cell Cycle Synchronization and Analysis—HC11 cells were synchronized by serum starvation for 48 h and were subsequently restimulated with growth medium containing 20% serum. At 4-h intervals, cells were trypsinized and washed in PBS, and approximately two-thirds of cells were pelleted and snap-frozen for subsequent protein harvest. The remaining cells were pelleted, resuspended in PBS, and fixed in 70% ethanol. Following fixation, cells were pelleted, resuspended in PBS supplemented with 10 μg/ml propidium iodide and 100 μg/ml RNase A, and sorted by DNA content using a Becton Dickinson FACScan flow cytometer. The program ModFit was used to quantify percentages of cells in each phase of the cell cycle.

Subcellular Fractionation—Nuclear and cytoplasmic fractionation was performed as described previously (34). Briefly, 16MB9A cells were harvested by trypsinization, pelleted, and washed in PBS. Cells were washed in ice-cold hypotonic buffer (30 mM HEPES, pH 7.5, 5 mM KCl, 1 mM $MgCl_2$), resuspended in three packed cellular volumes of hypotonic buffer supplemented with protease inhibitors, and incubated on ice for 30 min. Cells were homogenized in a Wheaton Dounce with 25 strokes of a type B pestle. An equal volume of Nonidet P-40 lysis buffer (0.1% Igepal CA-630, 250 mM sucrose, 1 mM $MgCl_2$, 10 mM Tris, pH 7.5) was added dropwise, and cells were lysed using another 10 strokes. Nuclei were pelleted at 1300 × *g* at 4 °C for 5 min. Following removal of the cytoplasmic supernatant, nuclei were washed twice in 1:1 hypotonic buffer/Nonidet P-40 lysis buffer and resuspended in an amount of 1:1 hypotonic buffer/Nonidet P-40 lysis buffer equal to the extract volume prior to centrifugation of nuclei. Nuclear and cytoplasmic fractions were diluted with 6× EBC to a final concentration of 1×, centrifuged to remove insoluble debris, and boiled in 1× (final) Laemmli sample buffer prior to SDS-PAGE.

Immunofluorescence—Cells were cultured in 2-well culture slides (Falcon), rinsed in PBS, and fixed for 10 min in 3% paraformaldehyde/2% sucrose/PBS. Cells were rinsed twice in PBS and permeabilized for 5 min in ice-cold buffer (0.5% Triton, 20 mM HEPES, pH 7.4, 50 mM NaCl, 3 mM $MgCl_2$, 300 mM sucrose). Following five rinses in PBS, cells were incubated at 37 °C for 20 min with anti-Brca2A (2 μg/ml in 3% bovine serum albumin/PBS). Cells were rinsed twice in PBS and

[1] The abbreviations used are: GST, glutathione *S*-transferase; PAGE, polyacrylamide gel electrophoresis; PBS, phosphate-buffered saline.

stained with a 1:200 dilution of fluorescein isothiocyanate-conjugated goat anti-rabbit IgG (Jackson Immunoresearch) in 3% bovine serum albumin/PBS. Stained cells were rinsed three times in PBS, mounted in Vectastain (Vector Laboratories), and visualized using a Bio-Rad MRC-1024 confocal microscope with a Kr/Ar laser. For subcellular localization of Brca2 isoforms, tetramethylrhodamine isothiocyanate-conjugated goat anti-rabbit (Jackson Immunoresearch) was used as a secondary antibody at a 1:200 dilution, and cells were visualized using confocal microscopy as above.

RESULTS

Generation of Antisera to Murine Brca2—To investigate the function of the murine Brca2 protein, we raised antisera to two recombinant Brca2 polypeptides corresponding to amino acid residues 19–135 and 206–566. Sera from these rabbits were affinity-purified and designated anti-Brca2A and anti-Brca2B, respectively. To demonstrate that these antibodies specifically recognize murine Brca2, we transfected 293T cells with either a full-length cDNA encoding *Brca2* or an empty vector control. Immunoblotting of whole cell extracts with anti-Brca2A demonstrated a band of the predicted molecular mass in 293T cells transfected with a *Brca2* cDNA but not in cells transfected with a control vector (Fig. 1*A*). This band co-migrates with endogenous Brca2 detected in the mammary epithelial cell lines HC11, NMuMG, and 16MB9A. Endogenous human BRCA2, detected in 293T cells using an antibody recognizing a carboxyl-terminal epitope of BRCA2, also co-migrates with this band (Fig. 1*A*). In contrast, no co-migrating band is detected by immunoblot of whole cell extracts from CAPAN-1 cells, in which a 6174dT frameshift mutation results in a carboxyl-terminal truncation of the *BRCA2* gene product (Fig. 1*A*). Detection of murine Brca2 was completely blocked by pre-incubating anti-Brca2A with the cognate GST-Brca2 (residues 19–135) fusion protein but not by pre-incubating with GST (data not shown). These findings indicate that anti-Brca2A specifically detects murine Brca2.

As further evidence of the specificity of anti-Brca2A, we performed reciprocal immunoprecipitations and immunoblots on murine mammary epithelial cell extracts with anti-Brca2A and anti-Brca2B. As shown in Fig. 1*B*, anti-Brca2A detects a polypeptide of the appropriate molecular mass present in cell extracts subjected to immunoprecipitation with anti-Brca2B but not with control rabbit IgG. Similarly, anti-Brca2B detects a polypeptide of the appropriate molecular mass in cell extracts subjected to immunoprecipitation with anti-Brca2A. Moreover, the polypeptide immunoprecipitated by anti-Brca2A and anti-Brca2B co-migrates with the polypeptides detected by these antibodies in whole cell extracts (see below, and see Fig. 4). In aggregate, these data demonstrate that anti-Brca2A and anti-Brca2B specifically recognize murine Brca2.

Brca2 Protein Levels Are Up-regulated during S and G_2/M Phases of the Cell Cycle—Our laboratory has demonstrated previously that steady-state levels of murine *Brca2* mRNA are regulated during the cell cycle with peak expression occurring near the G_1/S transition (35). Human BRCA2 has been shown to exhibit a similar pattern of regulation at both the RNA and protein levels (5, 6). To determine whether steady-state levels of murine Brca2 protein are similarly regulated, HC11 cells were synchronized by serum starvation for 48 h, restimulated with serum, and harvested at 4-h intervals. Immunoblotting revealed that murine Brca2 expression is up-regulated beginning at ~12 h following restimulation with serum, which coincides with cellular entry into S phase as shown both by flow cytometry and up-regulation of cyclin A (Fig. 2). This up-regulation persists as cells exit S phase and enter the G_2/M phase of the cell cycle (Fig. 2). Similar results were observed in a second mammary epithelial cell line, NMuMG (data not shown). These findings indicate that the cell cycle regulation of BRCA2 is conserved between mouse and human at both the RNA and protein level.

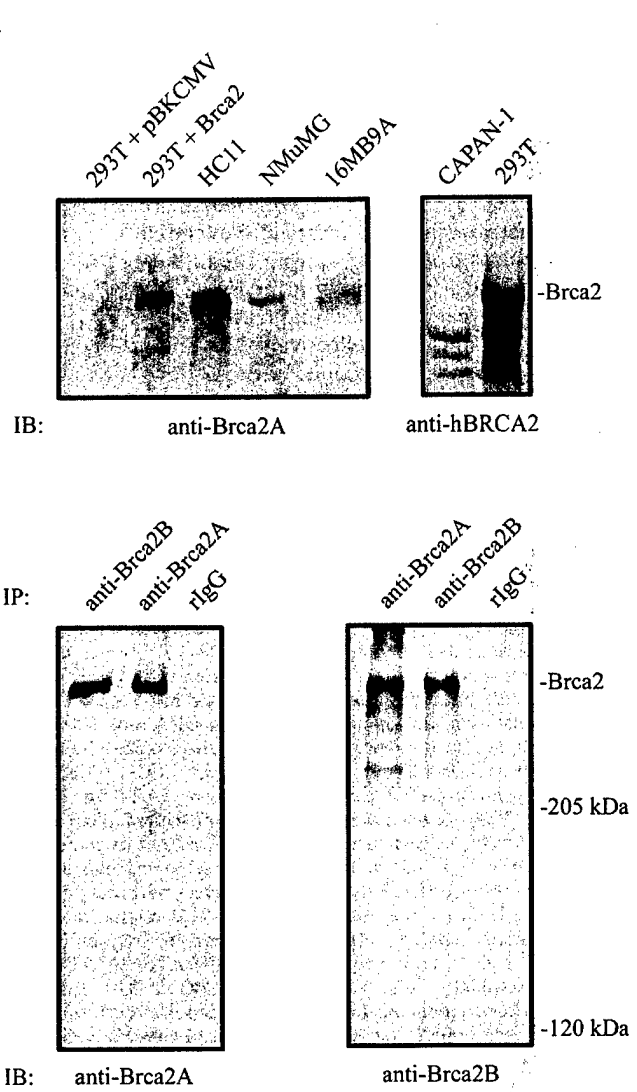

FIG. 1. **Characterization of Brca2 antibodies.** *A*, whole cell protein extracts were generated from 293T cells transiently transfected with a *pBKCMV* vector control or a *Brca2* expression plasmid or from murine mammary epithelial cell lines (HC11, NMuMG, and 16MB9A), the *BRCA2* mutant human pancreatic adenocarcinoma cell line CAPAN-1, or untransfected 293T cells. 60 μg (*lanes 1–3*) or 40 μg (*lanes 4–6*) of cell extracts were separated by SDS-PAGE and immunoblotted (*IB*) with anti-Brca2A (*left panel*) or anti-human BRCA2 Ab-2 (Oncogene Science; *right panel*) antibodies. *B*, Brca2 was immunoprecipitated (*IP*) from HC11 cells (*left panel*) or 16MB9A cells (*right panel*) using the indicated antibodies. Precipitates were separated by SDS-PAGE and immunoblotted with anti-Brca2A (*left panel*) or anti-Brca2B (*right panel*).

Murine Brca2 Localizes to Nuclear Foci—Human BRCA2 has been shown to localize to nuclei by biochemical subcellular fractionation (6). To determine whether murine Brca2 shares this property, nuclear and cytoplasmic fractions were prepared from the murine mammary epithelial cell line, 16MB9A. The purity of these fractions was confirmed by immunoblotting for β-tubulin and RAD50 as controls for cytoplasmic and nuclear proteins, respectively (Fig. 3*A*). This analysis demonstrated that murine Brca2 is found primarily in the nuclear fraction of 16MB9A cells (Fig. 3*A*).

Consistent with the nuclear localization of human BRCA2, immunofluorescence studies have shown that this protein localizes to subnuclear foci (16). To determine whether murine Brca2 exhibits a similar localization, we performed indirect

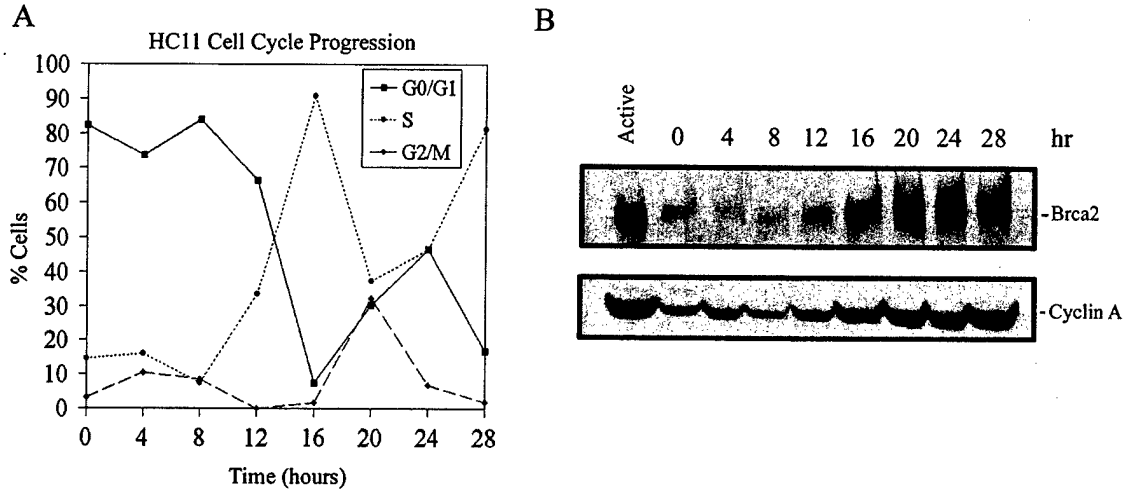

FIG. 2. **Murine Brca2 is cell cycle-regulated.** Serum-starved HC11 cells were stimulated to re-enter the cell cycle by refeeding with 20% serum, and cells were harvested at the indicated time points. *A*, histograms representing the DNA content of cells stained with propidium iodide and subjected to flow cytometry. The relative percentage of cells in different phases of the cell cycle was determined and plotted for each time point. *B*, whole cell extracts (50 μg) from synchronized HC11 cells were immunoblotted using anti-Brca2A or anti-cyclin A antibodies.

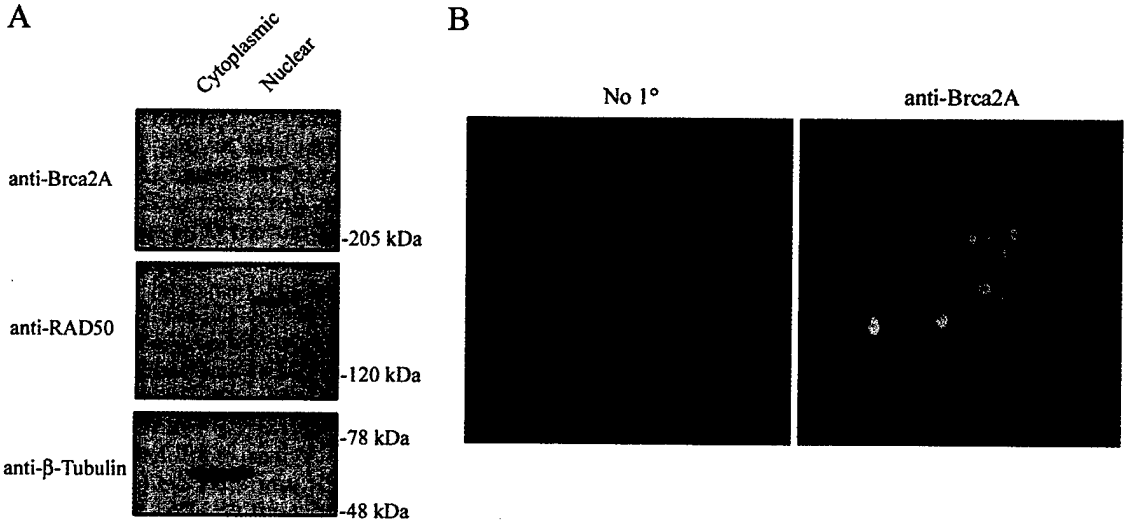

FIG. 3. **Brca2 is a nuclear protein that localizes to discrete foci in mitotic cells.** *A*, 16MB9A cells were separated into nuclear and cytoplasmic fractions, equal proportions of which were immunoblotted with anti-Brca2A, anti-RAD50 (a control nuclear protein), or anti-β-tubulin (a control cytoplasmic protein) antibodies. *B*, endogenous Brca2 was detected in asynchronously growing NMuMG cells by indirect immunofluorescence using anti-Brca2A (*right panel*). A control panel representing immunostaining performed without primary antibody is shown (*left panel*).

immunofluorescence on NMuMG cells using anti-Brca2A. Numerous nuclear foci were observed in cells stained with anti-Brca2A but not in cells stained with a secondary antibody alone (Fig. 3*B*). Fluorescent signal was completely blocked by the cognate GST-Brca2 (residues 19–135) fusion protein but not by GST alone (data not shown). Collectively, these data demonstrate that, similar to human BRCA2, murine Brca2 is a nuclear protein and localizes to discrete foci in mammary epithelial cell lines.

Brca2 Stably Interacts with Rad51 and Brca1—Human BRCA2 has been demonstrated previously to physically interact with the homology-based DNA repair protein, RAD51 (12–16). This interaction has been shown to be direct by both yeast two-hybrid and *in vitro* GST pulldown assays (12, 14, 15). Although murine Brca2-GST fusion proteins have been shown to bind to Rad51 *in vitro*, and murine Brca2-GAL4 fusion proteins have been shown to bind to Rad51 by yeast two-hybrid approaches (19, 32), endogenous murine Brca2 and Rad51 have yet to be shown to interact in mammary epithelial cells *in vivo*. To address this, we performed reciprocal co-immunoprecipitations of Rad51 and Brca2 from HC11 cells (Fig. 4*A*). This analysis demonstrated that Rad51 antisera were equally as effective as Brca2 antibodies in immunoprecipitating Brca2, suggesting that the majority of Brca2 in these cells is stably bound to Rad51. In contrast, Brca2 antisera co-immunoprecipitated only a fraction of the total Rad51 present in these cells (Fig. 4*A*). Consistent with this finding, a similarly small proportion of RAD51 has been found complexed with BRCA2 in human cells (13, 16). Together, these observations suggest that within cells there is a large pool of Rad51 molecules that are not complexed with Brca2. Although we cannot rule out the possibility that there is a significant pool of Brca2 molecules that are not immunoprecipitated by our Brca2 antibodies, this latter explanation appears unlikely given that anti-Brca2B antibodies immunoprecipitate the majority of Brca2 present in these cells as judged by comparison to input material (Fig. 4*A*).

Because human BRCA2 has also been demonstrated to interact with BRCA1 (16), we wished to determine whether an analogous interaction exists in murine cells. Using polyclonal antibodies raised against murine Brca1 residues 69–278 (mAb-1) and residues 995–1244 (mAb-3) (36), we performed reciprocal co-immunoprecipitations of Brca1 with Brca2. Low

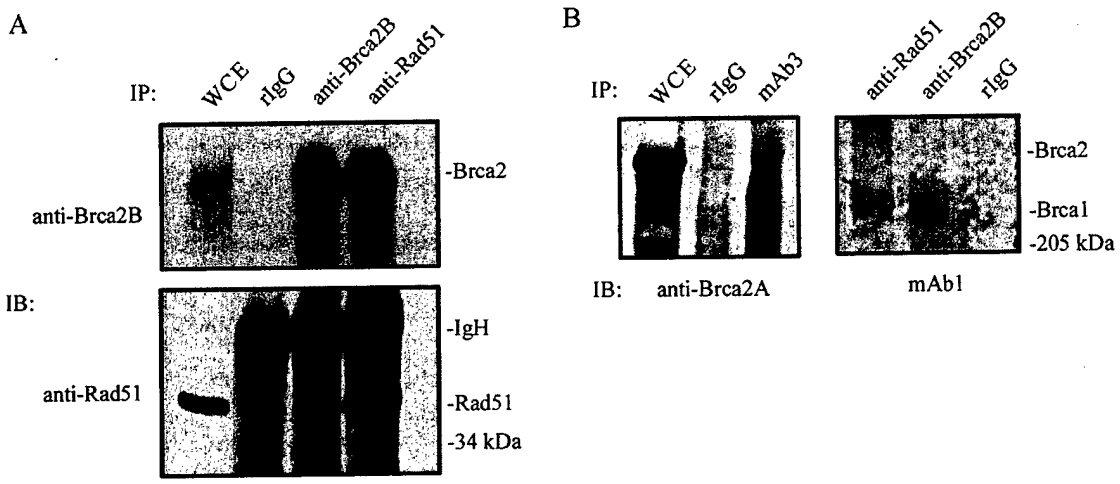

FIG. 4. **Brca2 interacts with Rad51 and with murine Brca1 *in vivo*.** *A*, asynchronously growing HC11 cells were harvested and immunoprecipitated using anti-Brca2B, anti-RAD51 Ab-1 (Oncogene Science), or rabbit IgG. Precipitates were separated by SDS-PAGE and immunoblotted with anti-Brca2A (*top panel*) or with anti-RAD51 Ab-1 (Oncogene Science; *bottom panel*). The whole cell extract (*WCE*) represents 1/30 of the input protein. *B*, Brca1 (*left panel*), Brca2 (*right panel*), or Rad51 (*right panel*) were immunoprecipitated (*IP*) from HC11 whole cell extracts using the indicated antibodies. Precipitates were immunoblotted (*IB*) with anti-Brca2A (*left panel*) or anti-Brca1 mAb-1 (*right panel*). The whole cell extract represents 1/20 of the input protein.

but significant levels of Brca2 were detected in Brca1 immunoprecipitates (Fig. 4*B*). Based on comparisons to input cellular extracts, less than 5% of total Brca2 polypeptides appear to be stably bound to Brca1 under these conditions (Fig. 4*B*). This finding is consistent with the fraction of total BRCA2 molecules that have been reported to be bound to BRCA1 in human cells (16). Conversely, we detected Brca1 in Brca2 immunoprecipitates at levels approximately equivalent to those present in Rad51 precipitates (Fig. 4*B*). No Brca1 or Brca2 was detected in rabbit IgG control precipitates. Taken together, our data indicate that the proteins with which murine Brca2 interacts are similar to those with which human BRCA2 interacts and that the stoichiometries with which these interactions occur may also be similar. Of note, however, we cannot rule out the possibility that our antibodies have incomplete access to cellular Brca2-Brca1 complexes or that the immunoprecipitation conditions employed in these experiments cause disruption of Brca2-Brca1 complexes.

Exon 11 of Murine Brca2, but Not Its Carboxyl Terminus, Is Required for Interaction with Rad51—The domain(s) with which murine and human BRCA2 each interact with RAD51 have been noted previously to differ (37). Specifically, murine Brca2 has been shown to interact with Rad51 via its carboxyl terminus by yeast two-hybrid and *in vitro* GST pulldown assays (19, 38). However, despite the high degree of evolutionary conservation of this domain, similar approaches have indicated that the corresponding domain of human BRCA2 does not stably interact with RAD51 (12, 14, 15). Rather, the BRC repeats of human BRCA2 have been shown to be necessary and sufficient for interaction with RAD51. To date, the contribution of the BRC repeats of murine Brca2 to its interaction with Rad51 have not been addressed. We generated several deletion mutants of *Brca2* to identify those domain(s) required for Rad51 interaction (Fig. 5*A*). The expression construct, *Brca2ΔBst*, contains an in-frame deletion of the majority of exon 11 that spans all 8 BRC repeats. *Brca2ΔC* contains a deletion of all *Brca2* sequences 3′ of exon 11, including the reported carboxyl-terminal Rad51 interaction domain (19, 38). Finally, *Brca2ΔBst-C* deletes both exon 11 and carboxyl-terminal sequences. Each of these constructs retains the epitopes recognized by anti-Brca2A and anti-Brca2B.

293T cells were transfected with expression constructs for full-length *Brca2*, *Brca2* deletion mutants, or a *pBKCMV* control vector, and harvested cell extracts were subjected to immunoprecipitation for Brca2 and RAD51. This analysis revealed that full-length Brca2 and Brca2ΔC were comparable in their ability to co-precipitate RAD51 (Fig. 5*B*). In contrast, no RAD51 was detected in anti-Brca2 immunoprecipitates from cells transfected with *Brca2ΔBst* or *Brca2ΔBst-C*, despite the fact that these Brca2 mutant polypeptides were expressed at levels that exceeded those of full-length Brca2 and Brca2ΔC (Fig. 5*B*). Performing the reciprocal co-immunoprecipitation experiment in 293T cells yielded similar results, as full-length Brca2 and Brca2ΔC were found to co-immunoprecipitate with RAD51, whereas Brca2ΔBst and Brca2ΔBst-C failed to co-precipitate with RAD51 (Fig. 5*C*). These results were also observed when Brca2ΔBst and Brca2ΔBst-C were expressed at levels comparable with those of full-length Brca2 and Brca2ΔC (data not shown) indicating that the failure of Brca2ΔBst and Brca2ΔBst-C to interact with RAD51 is not an artifact of their higher expression levels. Moreover, the fact that human and murine RAD51 are identical at the amino acid level, and that the BRCA2-RAD51 interaction has been shown to be direct, suggests that the inability of Brca2ΔBst and Brca2ΔBst-C to co-precipitate RAD51 is not due to differences in RAD51 sequences or bridging molecules present in human cells (12, 14, 15). Collectively, these data strongly suggest that exon 11 is the principal RAD51 interaction domain contained within murine Brca2.

The Amino Terminus of Murine Brca2 Is Sufficient for Interaction with Human BRCA1—Brca1 and Brca2 each display relatively low overall similarity to their human orthologs (~59%). Given this, we wished to define the domain(s) of Brca2 required for interaction with Brca1 and to determine whether the Brca2-Brca1 interaction would be preserved when one of these proteins was replaced by its human counterpart. Extracts of 293T cells transfected with full-length *Brca2* or *Brca2* deletion constructs, along with a *BRCA1* expression construct, were subjected to Brca2 immunoprecipitation and immunoblotted for co-precipitating BRCA1 (Fig. 6). This analysis revealed that each of the mutant Brca2 isoforms tested were comparable in their ability to interact with human BRCA1. Similar results were observed in co-immunoprecipitations performed using anti-Brca2A or anti-Brca2B and in the absence of ectopic BRCA1 expression (data not shown). Low levels of BRCA1 were detectable in anti-Brca2A precipitates from 293T cells transfected

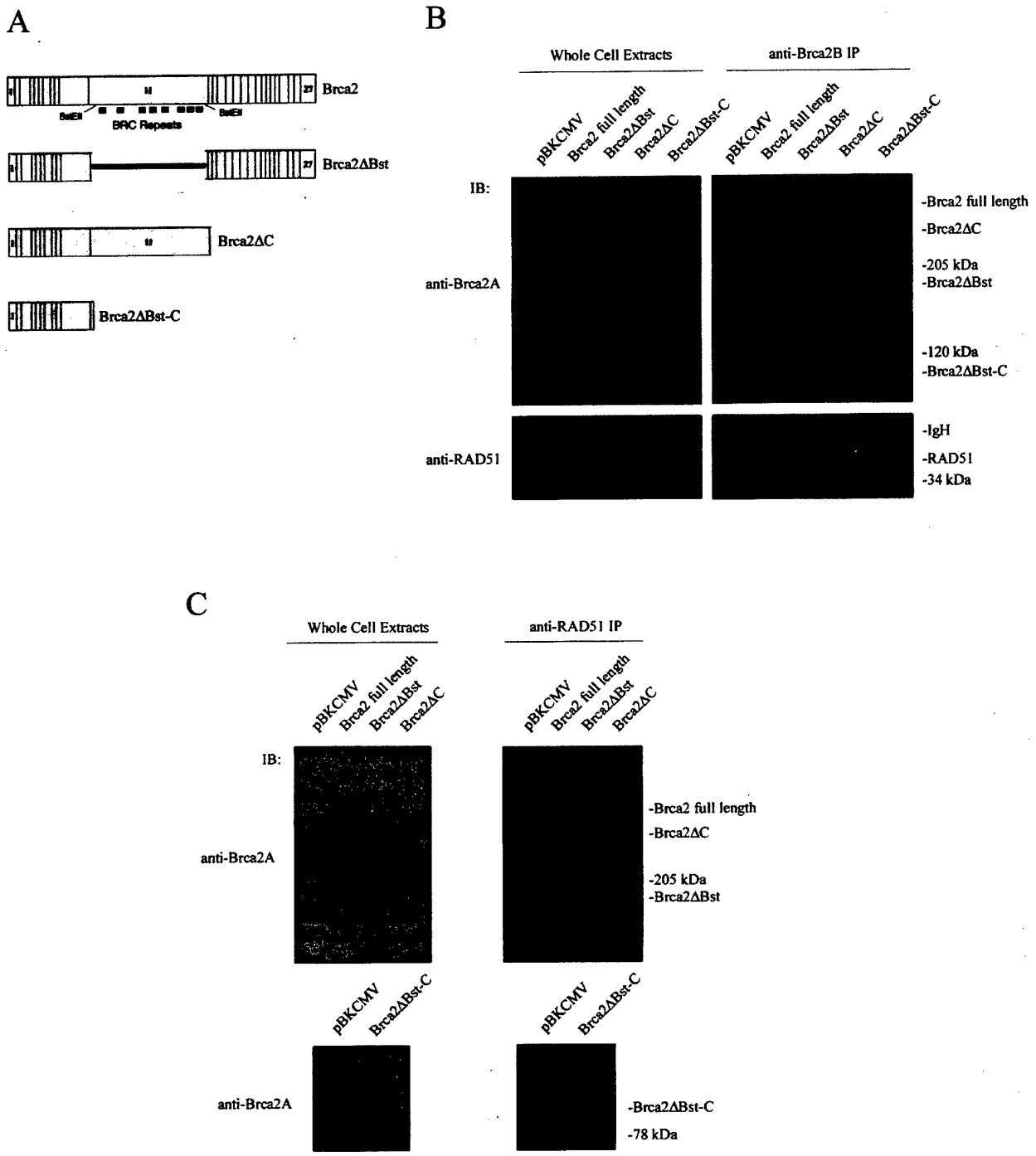

FIG. 5. **Exon 11, but not the carboxyl terminus, of murine Brca2 is required for interaction with RAD51.** *A*, schematic depicting deletion mutants of *Brca2* generated from a full-length *Brca2* cDNA. *Brca2ΔBst* represents an internal deletion mutant that encodes a polypeptide lacking amino acid residues 738–2278 from exon 11. *Brca2ΔC* lacks sequence from the second *Bst*EII site, at residue 2280, to the carboxyl terminus of the protein, and *Brca2ΔBst-C* lacks sequence from the first *Bst*EII site, at residue 742, to the carboxyl terminus of the protein. *B*, 293T cells were transfected with 25 μg of the indicated *Brca2* constructs. Cellular extracts (*left panels*) or cellular extracts immunoprecipitated (*IP*) with anti-Brca2B (*right panels*), were separated by SDS-PAGE and immunoblotted with either anti-Brca2A (*top panel*) or anti-RAD51 Ab-1 (NeoMarkers; *bottom panel*). *C*, 293T cells were transfected with 25 μg of the indicated *Brca2* constructs. Whole cell extracts (*left panels*) or whole cell extracts immunoprecipitated with anti-RAD51 Ab-1 (Oncogene Science; right panels) were immunoblotted (*IB*) with anti-Brca2A. The *bottom panels* were separated by 15 rather than 5% SDS-PAGE to enhance the resolution of Brca2ΔBst-C.

with the control vector, *pBKCMV*, suggesting that anti-Brca2A may cross-react, albeit weakly, with human BRCA2 (Fig. 6). In aggregate, our findings suggest that sequences within the amino-terminal 738 residues of Brca2 are sufficient for interaction with BRCA1, although additional domains of Brca2 may contribute to the stability of this association. These findings are consistent with experiments demonstrating that the interaction of human BRCA2 and BRCA1 is preserved in CAPAN-1 cells, which express a BRCA2 protein that lacks the carboxyl-terminal third of BRCA2 (16). To date, the lack of an antibody to the carboxyl terminus of Brca2 and inefficient expression of epitope-tagged Brca2 deletion mutants (data not shown) have prevented us from testing whether the amino terminus of Brca2 is required for its interaction with BRCA1. Nevertheless, we conclude that the amino terminus of murine Brca2 is sufficient to stably interact with human BRCA1 and that the se-

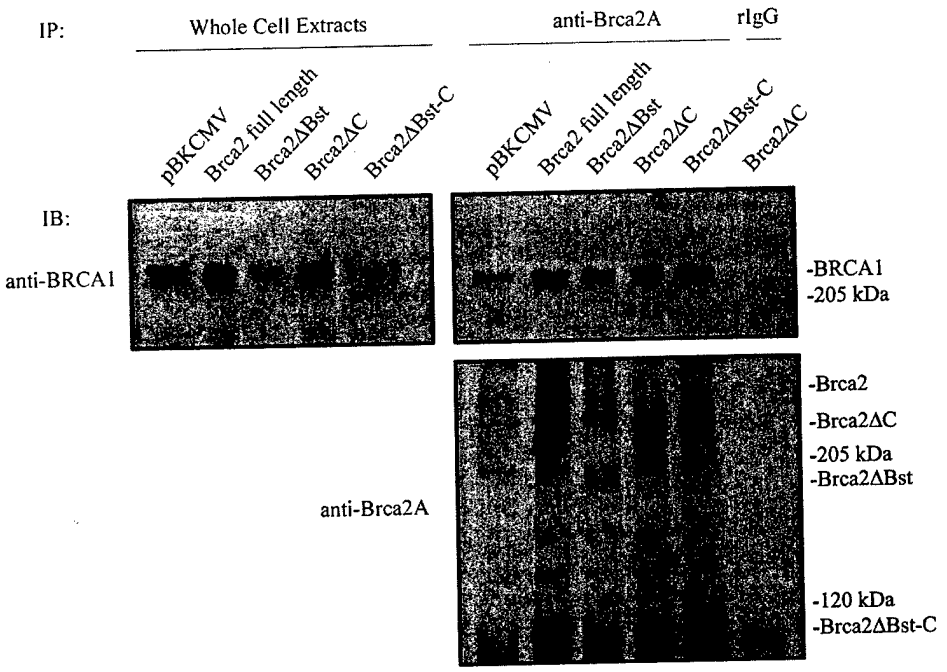

FIG. 6. **The amino terminus of Brca2 is sufficient for interaction with BRCA1.** 293T cells were transfected with 12.5 μg of *pBKCMV*, 12.5 μg of full-length *Brca2*, 2 μg of *Brca2ΔBst*, 12.5 μg of *Brca2ΔC*, or 2 μg of *Brca2ΔBst-C*. All transfections included 12.5 μg of a *BRCA1* expression plasmid and sufficient *pBKCMV* to bring the total DNA to 25 μg per transfection. Whole cell extracts (*left panel*) or anti-Brca2A immunoprecipitates (*right panels*) from transfected cells were immunoblotted (*IB*) with anti-BRCA1 MS110 (*top panels*) or anti-Brca2A (*bottom panel*). *IP*, immunoprecipitated.

quences mediating this interaction have been evolutionarily conserved.

The Amino Terminus of Murine Brca2 Is Sufficient for Nuclear Localization—Human BRCA2 has been shown to contain three nuclear localization signals at its extreme carboxyl terminus (3, 4). Accordingly, human *BRCA2* alleles that harbor truncating mutations anywhere within the gene result in BRCA2 polypeptides that localize to the cytoplasm and that are therefore presumed to be nonfunctional (3). If the signals directing nuclear localization in murine Brca2 are similarly positioned, even small carboxyl-terminal truncations in murine Brca2 should result in a cytoplasmic gene product. These findings predict that truncating mutations anywhere within *Brca2* would result in equally severe phenotypes. In contrast to this prediction, the viability of mice bearing truncations in *Brca2* directly correlates with the length of the resulting protein, in that amino-terminal truncations have more severe phenotypes than carboxyl-terminal truncations. We reasoned that it was more likely that murine and human BRCA2 would have conserved functions but different nuclear localization signal locations than have conserved nuclear localization signal locations and different functions. We tested this hypothesis using immunofluorescence to analyze the subcellular location of Brca2 polypeptides in 293T cells transiently transfected with the above murine *Brca2* deletion constructs.

As expected, exogenously expressed full-length murine Brca2 was observed to localize exclusively to the nucleus, as demonstrated by co-fluorescence with ECFP-Nuc (CLONTECH), a control for nuclear localization (Fig. 7). Similarly, Brca2ΔBst was also shown to localize to the nucleus of transfected cells, indicating that exon 11 is not required for the nuclear localization of murine Brca2. Surprisingly, Brca2ΔBst-C was also shown to localize to the nucleus despite its deletion of more than three-fourths of the full-length protein, including the carboxyl terminus. Brca2ΔBst-C encodes a polypeptide with a predicted molecular mass of 82 kDa that is significantly greater than the 65-kDa molecular mass cutoff for passive diffusion through nuclear pores (39). As such, the nuclear localization of Brca2ΔBst-C cannot be explained by simple diffusion. Moreover, no fluorescent signal was detected in control cells transfected with the empty vector, indicating that the apparent localization of Brca2ΔBst-C is not the result of antibody cross-reactivity with endogenous human BRCA2. These findings suggest that the amino terminus of murine Brca2 is sufficient to direct the nuclear localization of this protein.

DISCUSSION

We have demonstrated that the murine Brca2 protein is similar to human BRCA2 with regard to its nuclear localization, cell cycle regulation, binding to Brca1, and binding to Rad51. In addition, we have defined further the domains of Brca2 that are required for its interaction with RAD51 and BRCA1. Finally, despite low overall homologies between the murine and human orthologs of BRCA2 and BRCA1, we have demonstrated that murine Brca2 is capable of stably interacting with human BRCA1 *in vivo*. This indicates that the interaction between Brca1 and Brca2 has been conserved evolutionarily and suggests that this interaction is functionally important. In aggregate, our data are consistent with the hypothesis that murine and human BRCA2 have largely equivalent functions.

One notable difference that we observed between murine and human BRCA2 was the finding that the amino terminus of murine Brca2 appears to be sufficient for its nuclear localization. In contrast, analysis of human BRCA2-GFP fusion proteins has demonstrated that truncating even 155 residues from the carboxyl terminus of BRCA2 completely abrogates its nuclear localization (3). Similarly, endogenous BRCA2 in CAPAN-1 cells, which lacks the carboxyl-terminal third of BRCA2, has been shown to localize to the cytoplasm by biochemical fractionation (3). As such, we believe that our findings reflect differences in the placement of nuclear localization sequences within human and murine Brca2. A potential caveat to this interpretation is that our localization studies were performed on Brca2 polypeptides expressed ectopically in human 293T cells rather than in murine cells. However, our conclusions are supported by the finding that a targeted deletion of the final 566 coding nucleotides of *Brca2* results in a polypeptide that localizes to the nucleus in murine cells (40). Paradoxically, the difference in positioning of nuclear localization signals that we have identified between murine and human BRCA2 strengthens the hypothesis that murine and human BRCA2 are functionally equivalent. If, as for human BRCA2, truncation at the

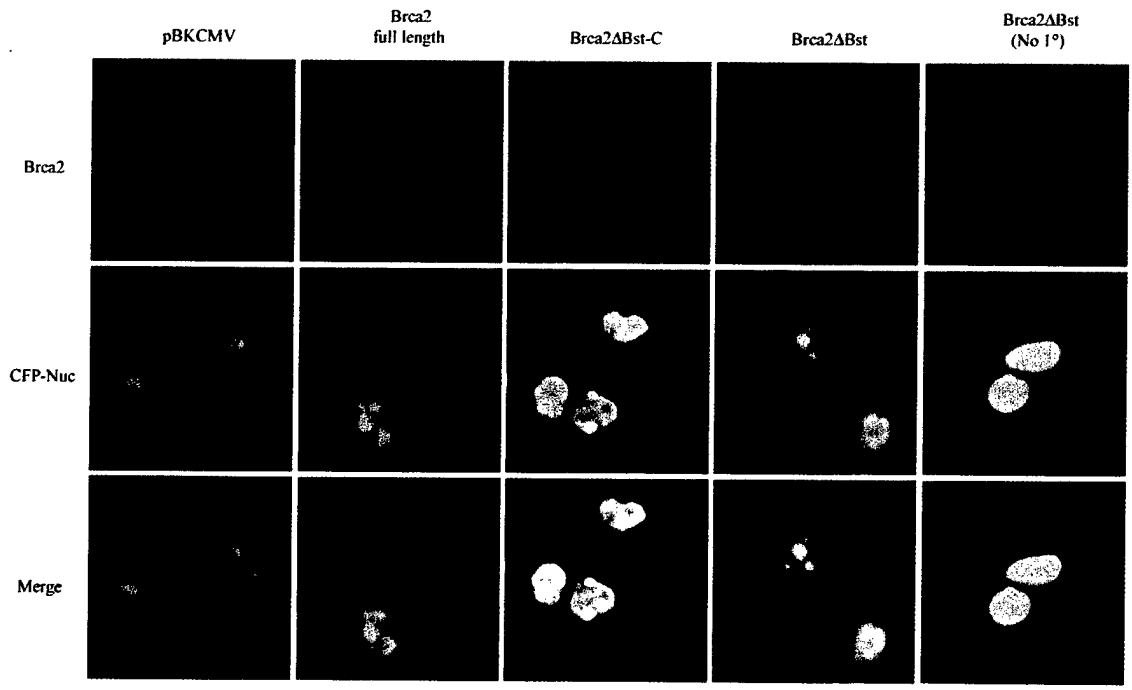

FIG. 7. **The amino terminus of murine Brca2 is sufficient for nuclear localization.** 293T cells were transiently transfected with 4.5 μg of the indicated *Brca2* deletion constructs and 0.5 μg of *pECFP-Nuc*. Cells were analyzed for Brca2 subcellular localization by indirect immunofluorescence with anti-Brca2A and co-fluorescence with CFP-Nuc.

extreme carboxyl terminus of murine Brca2 resulted in cytoplasmic localization, we would have been forced to conclude that the more severe phenotype of mice bearing amino-terminal compared with carboxyl-terminal truncating *Brca2* mutations reflected differences in the functions of murine and human BRCA2. Our demonstration that carboxyl-terminal truncations of murine Brca2 remain nuclear resolves this dilemma.

Mice homozygous for truncating mutations within exon 11 exhibit reduced embryonic survival, spontaneous tumorogenesis, genomic instability, and reduced Rad51 nuclear foci formation following DNA damage (27–30). Our finding that Brca2 polypeptides lacking exon 11 are incapable of co-immunoprecipitating RAD51 constitutes the first biochemical evidence that exon 11 is required for the interaction of Brca2 with RAD51. This, along with our observation that Brca2 mutants lacking the carboxyl terminus retain their capacity to bind to RAD51, is consistent with yeast two-hybrid studies of the human BRCA2-RAD51 interaction and suggests that exon 11 is the principal domain of murine Brca2 required for binding to RAD51. Nevertheless, given that interactions of the carboxyl terminus of murine Brca2 with Rad51 have been detected by two different approaches, we favor the possibility that this region may contribute to the interaction of Brca2 with Rad51. The targeted, in-frame deletion of exon 11 in mice would permit a more accurate assessment of the role of the BRC repeats in binding to Rad51 and of the impact that this interaction has on DNA repair and tumor susceptibility.

The multiple similarities between human and murine Brca2 that we have demonstrated in this report shed new light on observations made in mice bearing targeted mutations in *Brca2*. Mice lacking the small carboxyl-terminal domain of Brca2 shown to interact with Rad51 have not been reported to develop tumors, although cells from such mice exhibit premature senescence and decreased efficiency in homology-based DNA repair (31, 40). Our data predict that mice bearing carboxyl-terminal deletions would have at most only slightly impaired binding of Brca2 to Rad51. This, in turn, may explain the more modest phenotype of mice bearing such mutations. In support of this hypothesis, Moynahan and colleagues (40) have shown recently that the amount of Brca2 bound to Rad51 in murine embryonic stem cells is unaffected by deletion of the carboxyl-terminal domain of *Brca2*. As such, the premature senescence and decreased DNA repair phenotypes observed in these mice may be due either to an uncharacterized defect in the Rad51 pathway or to the disruption of interactions with other proteins involved in homology-based DNA repair.

Finally, our finding that the amino terminus of Brca2 is sufficient to interact with BRCA1 suggests that Brca2-Brca1 complexes may be maintained in all *Brca2* knockout mouse models generated to date; however, whether such Brca2-Brca1 complexes retain their function is unknown. Both *Brca2* and *Brca1* mutant cells have defects in Rad51 focus formation following DNA damage (36, 41). We have recently demonstrated that murine Brca1, like murine Brca2, localizes to nuclear foci (36). As peptides bearing consensus BRC repeat sequences can inhibit the polymerization of RAD51 onto DNA substrates *in vitro* (42), these data collectively suggest a role for Brca2, and potentially Brca1, in recruiting or preparing Rad51 for subsequent recombination events at sites of DNA damage. Nevertheless, it has yet to be demonstrated how Brca2 and Brca1 orchestrate Rad51 nuclear focus formation following DNA damage, and it has not been determined whether the disrupted regulation of Rad51 nuclear focus formation is ultimately responsible for the malignant transformation of *Brca1* and *Brca2* mutant cells. Such studies should enhance our understanding of the mechanism by which *Brca1* and *Brca2* gene products suppress tumor formation.

Acknowledgments—We thank Sherry M. Wang and Edward J. Gunther for provision of murine *Brca2* clones for use in the isolation of the *Brca2* cDNA. We also thank James Sanzo, Neelima Shah, and Irina Chernysh of the University of Pennsylvania Biomedical Imaging Core Laboratory for assistance with confocal microscopy and Hank Pletcher of the University of Pennsylvania Flow Cytometry and Cell Sorting Shared Resource Facility for assistance with FACS analysis.

REFERENCES

1. Ford, D., Easton, D. F., Stratton, M., Narod, S., Goldgar, D., Bishop, D. T., Weber, B., Lenoir, G., Chang-Claude, J., Sobol, H., Teare, M. D., Struewing, J., Arason, A., Scherneck, S., Peto, J., Rebbeck, T. R., Tonin, P., Neuhausen, S., Barkardottir, R., Eyfjord, J., Lynch, H., Ponder, B. A., Gayther, S. A., Zelada-Hedman, M., *et al.* (1998) *Am. J. Hum. Gen.* **62,** 676–689
2. Wooster, R., Bignell, G., Lancaster, J., Swift, S., Seal, S., Mangion, J., Collins, N., Gregory, S., Gumbs, C., and Micklem, G. (1995) *Nature* **378,** 789–792
3. Spain, B. H., Larson, C. J., Shihabuddin, L. S., Gage, F. H., and Verma, I. M. (1999) *Proc. Natl. Acad. Sci. U. S. A.* **96,** 13920–13925
4. Yano, K., Morotomi, K., Saito, H., Kato, M., Matsuo, F., and Miki, Y. (2000) *Bioch. Biophys. Res. Commun.* **270,** 171–175
5. Vaughn, J. P., Cirisano, F. D., Huper, G., Berchuck, A., Futreal, P. A., Marks, J. R., and Iglehart, J. D. (1996) *Cancer Res.* **56,** 4590–4594
6. Bertwistle, D., Swift, S., Marston, N. J., Jackson, L. E., Crossland, S., Crompton, M. R., Marshall, C. J., and Ashworth, A. (1997) *Cancer Res.* **57,** 5485–5488
7. Vaughn, J. P., Davis, P. L., Jarboe, M. D., Huper, G., Evans, A. C., Wiseman, R. W., Berchuck, A., Iglehart, J. D., Futreal, P. A., and Marks, J. R. (1996) *Cell Growth Differ.* **7,** 711–715
8. Chen, Y., Farmer, A. A., Chen, C. F., Jones, D. C., Chen, P. L., and Lee, W. H. (1996) *Cancer Res.* **56,** 3168–3172
9. Ruffner, H., and Verma, I. M. (1997) *Proc. Natl. Acad. Sci. U. S. A.* **94,** 7138–7143
10. Gudas, J. M., Li, T., Nguyen, H., Jensen, D., Rauscher, F. J., III, and Cowan, K. H. (1996) *Cell Growth Differ.* **7,** 717–723
11. Chen, F., Nastasi, A., Shen, Z., Brenneman, M., Crissman, H., and Chen, D. J. (1997) *Mutat. Res.* **384,** 205–211
12. Chen, P. L., Chen, C. F., Chen, Y., Xiao, J., Sharp, Z. D., and Lee, W. H. (1998) *Proc. Natl. Acad. Sci. U. S. A.* **95,** 5287–5292
13. Marmorstein, L. Y., Ouchi, T., and Aaronson, S. A. (1998) *Proc. Natl. Acad. Sci. U. S. A.* **95,** 13869–13874
14. Wong, A. K. C., Pero, R., Ormonde, P. A., Tavtigian, S. V., and Bartel, P. L. (1997) *J. Biol. Chem.* **272,** 31941–31944
15. Katagiri, T., Saito, H., Shinohara, A., Ogawa, H., Kamada, N., Nakamura, Y., and Miki, Y. (1998) *Genes Chromosomes Cancer* **21,** 217–222
16. Chen, J. J., Silver, D. P., Walpita, D., Cantor, S. B., Gazdar, A. F., Tomlinson, G., Couch, F. J., Weber, B. L., Ashley, T., Livington, D. M., and Scully, R. (1998) *Mol. Cell* **2,** 317–328
17. Bork, P., Blomberg, N., and Nilges, M. (1996) *Nat. Genet.* **13,** 22–23
18. Bignell, G., Micklem, G., Stratton, M. R., Asworth, A., and Wooster, R. (1997) *Hum. Mol. Genet.* **6,** 53–58
19. Sharan, S. K., Morimatsu, M., Albrecht, U., Lim, D. S., Regel, E., Dinh, C., Sands, A., Eichele, G., Hasty, P., and Bradley, A. (1997) *Nature* **386,** 804–810
20. Suzuki, A., de la Pompa, J. L., Hakem, R., Elia, A., Yoshida, R., Rong, M., Nishina, H., Chuang, T., Wakeham, A., Itie, A., Koo, W., Billia, P., Ho, A., Fukumoto, M., Hui, C. C., and Mak, T. W. (1997) *Genes Dev.* **11,** 1242–1252
21. Ludwig, T., Chapman, D. L., Papioannou, V. E., and Efstradiatis, A. (1997) *Genes Dev.* **11,** 1226–1241
22. Tsuzuki, T., Fujii, Y., Sakumi, K., Tominaga, Y., Nakao, K., Sekiguchi, M., Matsushiro, A., Yoshimura, Y., and Morita, T. (1996) *Proc. Natl. Acad. Sci. U. S. A.* **93,** 6236–6240
23. Gowen, L. C., Johnson, B. L., Latour, A. M., Sulik, K. K., and Koller, B. H. (1996) *Nat. Genet.* **12,** 191–194
24. Hakem, R., de la Pompa, J. L., Sirard, C., Mo, R., Woo, M., Hakem, A., Wakeham, A., Potter, J., Reitmair, A., Billia, F., Firpo, E., Hui, C. C., Roberts, J., Rossant, J., and Mak, T. W. (1996) *Cell* **85,** 1009–1023
25. Lim, D. S., and Hasty, P. (1996) *Mol. Cell. Biol.* **16,** 7133–7143
26. Hakem, R., de la Pompa, J. L., Elia, A., Potter, J., and Mak, T. W. (1997) *Nat. Genet.* **16,** 298–302
27. Connor, F., Bertwistle, D., Mee, P. J., Ross, G. M., Swift, S., Grigorieva, E., Tybulewicz, V. L. J., and Ashworth, A. (1997) *Nat. Genet.* **17,** 423–430
28. Friedman, L. S., Thistlewaite, F. C., Patel, K. J., Yu, V. P. C. C., Lee, H., Venkitaraman, A. R., Abel, K. J., Carlton, M. B. L., Hunter, S. M., Coledge, W. H., Evans, M. J., and Ponder, B. A. J. (1998) *Cancer Res.* **58,** 1338–1343
29. Patel, K., Yu, V. P. C. C., Lee, H., Corcoran, A., Thistlewaite, F. C., Evans, M. J., Colledge, W. H., Friedman, L. S., Ponder, B. A. J., and Venkitaraman, A. R. (1998) *Mol. Cell* **1,** 347–357
30. Yu, V. P., Koehler, M., Steinlein, C., Schmid, M., Hanakahi, L. A., van Gool, A. J., West, S. C., and Venkitaraman, A. R. (2000) *Genes Dev.* **14,** 1400–1406
31. Morimatsu, M., Donoho, G., and Hasty, P. (1998) *Cancer Res.* **58,** 3441–3447
32. Harlow, E., and Lane, D. (1988) *Antibodies: A Laboratory Manual*, 1st Ed., pp. 313–318, Cold Spring Harbor Laboratory Press, Cold Spring Harbor, NY
33. Ausubel, F. M., Brent, R., Kingston, R. E., Moore, D. D., Seidman, J. G., Smith, J. A., and Struhl, K. (2000) *Current Protocols in Molecular Biology*, 2nd Ed., pp. 9.1.4–9.1.6, John Wiley & Sons, Inc., New York
34. Wilson, C. A., Ramos, L., Villasenor, M. R., Anders, K. H., Press, M. F., Clarke, K., Karlan, B., Chen, J. J., Scully, R., Livingston, D., Zuch, R. H., Kanter, M. H., Cohen, S., Calzone, F. J., and Slamon, D. J. (1999) *Nat. Genet.* **21,** 236–240
35. Rajan, J. V., Wang, M., Marquis, S. T., and Chodosh, L. A. (1996) *Proc. Natl. Acad. Sci. U. S. A.* **93,** 13078–13083
36. Huber, L. J., Yang, T. W., Sarkisian, C. J., Master, S. R., Deng, C. X., and Chodosh, L. A. (2001) *Mol. Cell. Biol.* **21,** 4005–4015
37. Baer, R., and Lee, W. H. (1998) *J. Mammary Gland Biol. Neoplasia* **3,** 403–412
38. Mizuta, R., LaSalle, J. M., Cheng, H.-L., Shinohara, A., Ogawa, H., Copeland, N., Jenkins, N. A., LaLande, M., and Alt, F. W. (1997) *Proc. Natl. Acad. Sci. U. S. A.* **94,** 6927–6932
39. Gorlich, D., and Mattaj, I. W. (1996) *Science* **271,** 1513–1518
40. Moynahan, M. E., Pierce, A. J., and Jasin, M. (2001) *Mol. Cell* **7,** 263–272
41. Bhattacharyya, A., Ear, U. S., Koller, B. H., Weichselbaum, R. R., and Bishop, D. K. (2000) *J. Biol. Chem.* **275,** 23899–23903
42. Davies, A. A., Masson, J.-Y., Mcllwraith, M. J., Stasiak, A. Z., Stasiak, A., Venkitaraman, A. R., and West, S. C. (2001) *Mol. Cell* **7,** 273–282